Time Series Analysis: Gulf of Mexico Sea Level Rise

Dana Laufer

June 4, 2021

1 Abstract

In this study, I address the pressing issue of sea level rise, focusing specifically on the Gulf of Mexico. I examine the patterns of sea level rise in the Gulf by investigating monthly data from 1993 to 2020, identify a time series model that accurately represents these patterns, and finally use this model to predict the changes in the Gulf of Mexico sea level for the next 10 years. Using the small-sample corrected Akaike Information Criterion (AICc), I identify two suitable models to represent the data: SARIMA$(0, 1, 1), (0, 1, 1)_{12}$ and SARIMA$(1, 1, 1), (0, 1, 1)_{12}$. After performing diagnostic checking, I find that the first model fails the McLeod-Li Portmanteau Test for nonlinear dependence. Therefore, I choose SARIMA$(1, 1, 1), (0, 1, 1)_{12}$ as the most suitable model, and use this model to forecast data 10 years ahead. From this forecast, I conclude that in the next ten years, the sea level in the Gulf of Mexico is estimated to increase by just over 77 millimeters, which is slightly more than 3 inches.

2 Introduction

Climate change is a pressing matter for many reasons, one of which is the rising sea level. As temperatures rise, glaciers melt more in the summer than they can make up for in the winter, and this melted water increases the sea level. In addition, the water in the oceans absorb more heat as temperatures rise, causing the water to expand and increase the overall volume, and thus height, of the sea water. These rising sea levels can have catastrophic effects, and just a small increase can destroy coastal habitats for fish and birds, erode land, destroy cities, and strengthen hurricanes and typhoons. [2] Because of this, it is incredibly important to be able to predict the trajectory of the sea level in coming years, so that we may better prepare to deal with the consequences and attempt to mitigate the effects.

As sea levels rise, the Gulf of Mexico, although a somewhat small body of water compared to the Pacific and Atlantic oceans, threatens millions of people in Florida, Mississippi, Alabama, Louisiana and Texas. [3] Further, because it is a smaller body of water, its sea level has much less variability at any given time than other bodies of water, which means that predicted values of its mean sea level are more informative and valuable than others would be. For this reason, I will be modelling the sea level change in the Gulf of Mexico.

In this report, I use data that estimates the sea level change in the Gulf of Mexico from 1993 to 2020 using satellite radar altimeters. This altimetry data are provided by the NOAA Laboratory for Satellite Altimetry. By fitting a seasonal autoregressive moving average time series model, I predict that in the next 10 years, the mean sea level will increase by over 3 inches.

3 Data Preparation

3.1 Consolidation

The dataset I use in this report contains data on the change in mean sea level of the Gulf of Mexico from the beginning of 1993 to October 2020. The data points are estimated based on measurements from one of four different satellite radar altimeters: TOPEX/Poseidon (T/P), Jason-1, Jason-2, and Jason-3. There are five total variables in the dataset: a year variable, sorted in increasing order, containing real numbers that indicate the exact time that the data point was collected, and a column for each separate satellite radar altimeter. Most time points only contain an estimate from a single satellite, although some points contain estimates from multiple satellites. In order to simplify the dataset into a single sea level measurement, I take the mean of the four satellite radar altimeter estimates, ignoring missing values.

3.2 Linear Interpolation

After taking the mean across the four satellite estimates, I have a dataset with a year variable and a change in mean sea level variable. However, the data is still not prepared for standard, simple time series methods. This is because the dataset does not contain evenly spaced values: rather than containing daily, monthly, or yearly data, it appears that the data was recorded somewhat sporadically, possibly due to the nature of the satellite radar altimeters. Each year contains around 30 to 35 data points: more than monthly data would contain, but less than weekly or daily data. In order to correct this problem, I decided to use linear interpolation to find 12 evenly spaced data points for each year, that I could then treat as monthly data points. This seemed to be a more appropriate solution than taking the average of each month's data because of the nature of the data. The dataset tracks the mean change in sea level, which in reality changes fairly gradually, rather than changing sharply from one day to the next. Therefore, if we want to estimate the sea level value at any given time point, it seems appropriate that the value should be somewhere in between the observed value that was recorded just before the time point, and the observed value that was recorded just after it.

So, to create an evenly spaced dataset, I create a dataframe with a sea level variable full of missing values and a year variable with evenly spaced values, such that each year is divided into 12. The first year value is 1993, because the raw data starts at the very end of 1992, and the last year value is 2020.75, because the raw data ends at 2020.76. Then, for each year value in the evenly spaced dataset, a sea level value is estimated from the raw data by applying linear interpolation to the two observed sea level values closest in time to the year value in question.

In order to ensure that the coerced dataset is appropriate to use in place of the raw data, I compare plots and histograms of the two time series (Figures 1 and 2 in the Appendix), which confirms that the two series are extremely similar in general distribution and trend. Therefore, I am left with a dataset that contains estimated monthly sea level change values, which I can use standard time series methods on to estimate the raw time series data.

3.3 Transformations

Before moving forward, I split the even time series data into a training and testing set, reserving 50 data points in the testing set that I can use to test the accuracy of my final model.

Next, I investigate the plot of the even data to determine if any transformations are necessary. From the plot of the even time series (Right Side of Figure 1), there does not appear to be any severe change in variance across time. However, the histogram (Right Side of Figure 2) does indicate that the data is not entirely symmetrical. Therefore, a Boxcox transformation is fit to see if it improves the data. The data is first translated upwards so that all values are positive, then transformed such that $Y_t = \frac{1}{\lambda}(X_t^\lambda - 1)$, where X_t is the positive even data. I use a λ value of 0.707, which is obtained as the ideal value from the boxcox() function in R. Then, I compare plots and histograms of the even time series and the Boxcox transformed time series (Figures 3 and 4). These plots do not indicate much, if any, improvement in the variance or symmetry of the data, so I will proceed using the non-transformed data for ease of forecasting.

3.4 Differencing

Based on the plot of the even time series (Right Side of Figure 1), there is a definite upward trend in the data, suggesting that a differencing at lag 1 will likely be necessary. After differencing at lag 1, the variance decreases from 3,000 to 1,182, confirming that this did not over difference the data. Next, I examine the sample autocorrelation (ACF) and partial autocorrelation (PACF) of the data (Figure 5) to determine if any further differencing is needed. The ACF of the data decays very slowly and is highly dependent on the seasonality, which indicates that a differencing at lag 12 is required. This differencing decreases the variance from 1,182 to 927, confirming that the differencing was necessary. A third differencing, both at lag 1 and lag 12, is tried, but both greatly increase the variance of the data, indicating over differencing. Therefore, it seems that the data is stationary as is. Indeed, a plot of the data, pictured below, exhibits a constant mean, no linear trend, and no noticeable changes in variance. So, now that we have stationary data, we can move on to model identification.

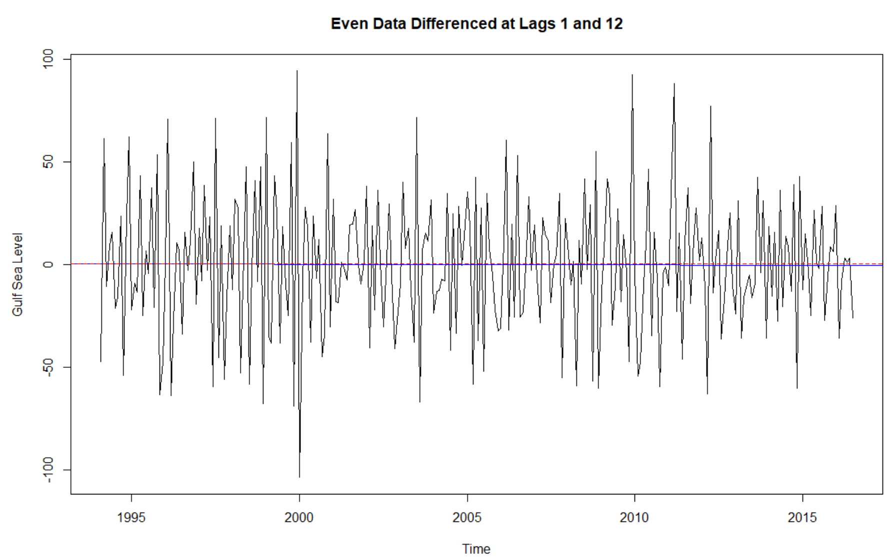

Figure 1: Plot of the stationary, evenly spaced data, with the linear trend drawn in red and the overall mean drawn in blue.

4 Model Identification

Based on the differencing of the data, we already know that the SARIMA model should have a period of 12, a nonseasonal differencing of 1 (d=1), and a seasonal differencing of 1 (D=1). However, we still need to determine appropriate values for p, q, P, and Q. In order to identify possible candidate models, I plot the ACF and PACF of the stationary data, pictured below.

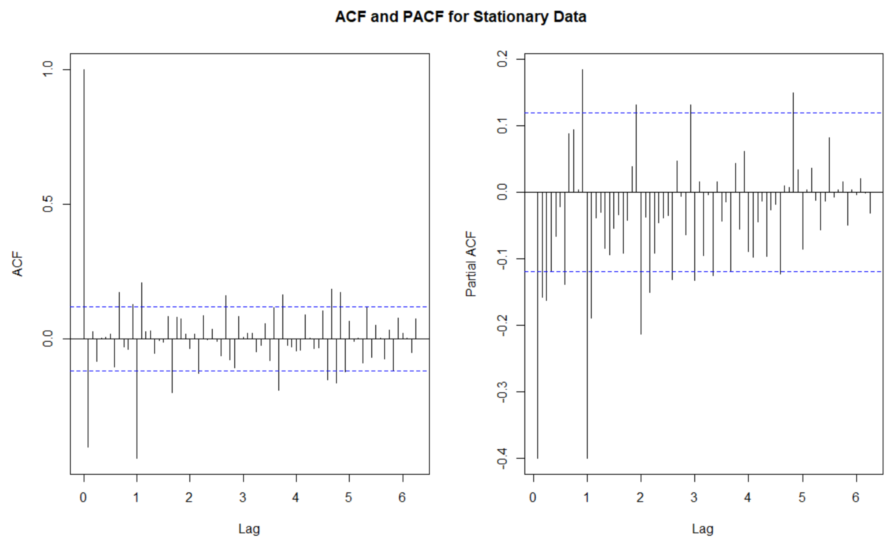

Figure 2: Side by side plots of the sample autocorrelation and sample partial autocorrelation of the stationary data, where each tick in the x axis indicates a multiple of 12.

The ACF has large spikes at lags 1 and 12, suggesting an MA and SMA order of 1. Further, the PACF also has large spikes at lags 1 and 12, again suggesting an AR and SAR order of 1. However, there are also very significant spikes in the PACF at lags 2, 3, 11, 13, and 24. This suggests a possible AR order of 3 and SAR order of 2. Based on these findings, I fit a number of SARIMA models, accounting for every possible combination of model with MA order up to 1 (q=1), SMA order up to 1 (Q=1), AR order up to 3 (p=3), and SAR order up to 2 (P=2), calculating the AICc for each model. From this, I investigate the four models with the lowest AICc, using R to estimate each coefficient's value and standard error. Then, using the fact that $\hat{\beta} \pm 1.96(se(\hat{\beta}))$ forms a 95% confidence interval for each coefficient, I investigate the significance of each coefficient, where I assume a coefficient is not statistically significant if its 95% confidence interval includes zero. In addition, I plot the roots of the characteristic polynomials of the models to determine stationarity and invertibility, where all moving average roots must lie outside of the unit circle to ensure invertibility, and all autoregressive roots must lie outside of the unit circle to ensure stationarity.

The coefficients of the first model, SARIMA$(0,1,1),(0,1,1)_{12}$, are both statistically significant, as can be seen below. Further, using the plot.roots.R function [1], we see that the nonseasonal roots of the model are all outside of the unit circle (Figure 6). Further, although the value of the SMA1 coefficient is quite close to -1 (which would produce a root of 1, violating the conditions for invertibility), the 95% confidence intervals do not include -1, so we can assume that the model is safely invertible.

$\text{SARIMA}(0,1,1),(0,1,1)_{12}$			
Coefficient	Coefficient Estimate	Lower Limit	Upper Limit
MA1	-0.6135	-0.7307	-0.4963
SMA1	-0.8032	-0.9036	-0.7028

Similarly, the coefficients of the second model, $\text{SARIMA}(1,1,1),(0,1,1)_{12}$, are all statistically significant, as can be seen below, and the nonseasonal roots of the model are all outside of the unit circle (Figures 7 and 8). Further, although the values of the SMA1 and MA1 coefficients are again quite close to -1, neither of the 95% confidence intervals do not include -1, so we can assume that the model is safely invertible.

$\text{SARIMA}(1,1,1),(0,1,1)_{12}$			
Coefficient	Coefficient Estimate	Lower Limit	Upper Limit
AR1	0.2579	0.0274	0.4884
MA1	-0.7994	-0.9725	-0.6263
SMA1	-0.8149	-0.9111	-0.7187

Examining the third model, $\text{SARIMA}(0,1,1),(1,1,1)_{12}$, we see that the SAR1 coefficient is not statistically significant. Setting this to zero, we obtain the first model, which has a lower AICc. So, we will no longer consider the $\text{SARIMA}(0,1,1),(1,1,1)_{12}$ in our model selection.

$\text{SARIMA}(0,1,1),(1,1,1)_{12}$			
Coefficient	Coefficient Estimate	Lower Limit	Upper Limit
MA1	-0.6101	-0.7280	-0.4923
SMA1	-0.8229	-0.9474	-0.6984
SAR1	0.0390	-0.1238	0.2017

Finally, looking at the fourth model, $\text{SARIMA}(3,1,1),(1,1,1)_{12}$, we can see that the 95% confidence interval for the MA1 coefficient includes -1, which would produce a root of 1, violating the conditions for invertibility. Further, the AR3 coefficient is not statistically significant. Setting this to zero, we obtain $\text{SARIMA}(2,1,1),(0,1,1)_{12}$, which has a lower AICc. However, the confidence interval of the MA1 coefficient still includes -1. Therefore, we will not consider either of these models in our model selection.

$\text{SARIMA}(3,1,1),(0,1,1)_{12}$			
Coefficient	Coefficient Estimate	Lower Limit	Upper Limit
AR1	0.3897	0.2568	0.5226
AR2	0.1505	0.01624	0.2848
AR3	0.0436	-0.0832	0.1704
MA1	-0.9587	-1.0242	-0.8932
SMA1	-0.7904	-0.8966	-0.6842

SARIMA$(2,1,1),(0,1,1)_{12}$			
Coefficient	Coefficient Estimate	Lower Limit	Upper Limit
AR1	0.3885	0.2501	0.5269
AR2	0.1600	0.0253	0.2947
MA1	-0.9506	-1.0237	-0.8775
SMA1	-0.7924	-0.8996	-0.6852

5 Diagnostic Checking

We now have two models to perform diagnostic checking on: SARIMA$(0,1,1),(0,1,1)_{12}$ and SARIMA$(1,1,1),(0,1,1)_{12}$, which I will now refer to as Model 1 and Model 2 respectively. If a model fits the data well, the residuals should resemble Gaussian white noise. First, I produce plots of the residuals of both models with the linear trend and mean superimposed (Figure 9), which both indicate fairly stationary data, with constant mean and variance. Next, I plot histograms of the residuals with a normal curve superimposed (Figures 10 and 11), which both display fairly symmetrical and normal data. Further, plots of the ACF and PACF of both residuals, shown below, indicate white noise data, with all values within the 95% confidence intervals, and the ar() function in R selects an AR(0) model, or a white noise model, for both residuals.

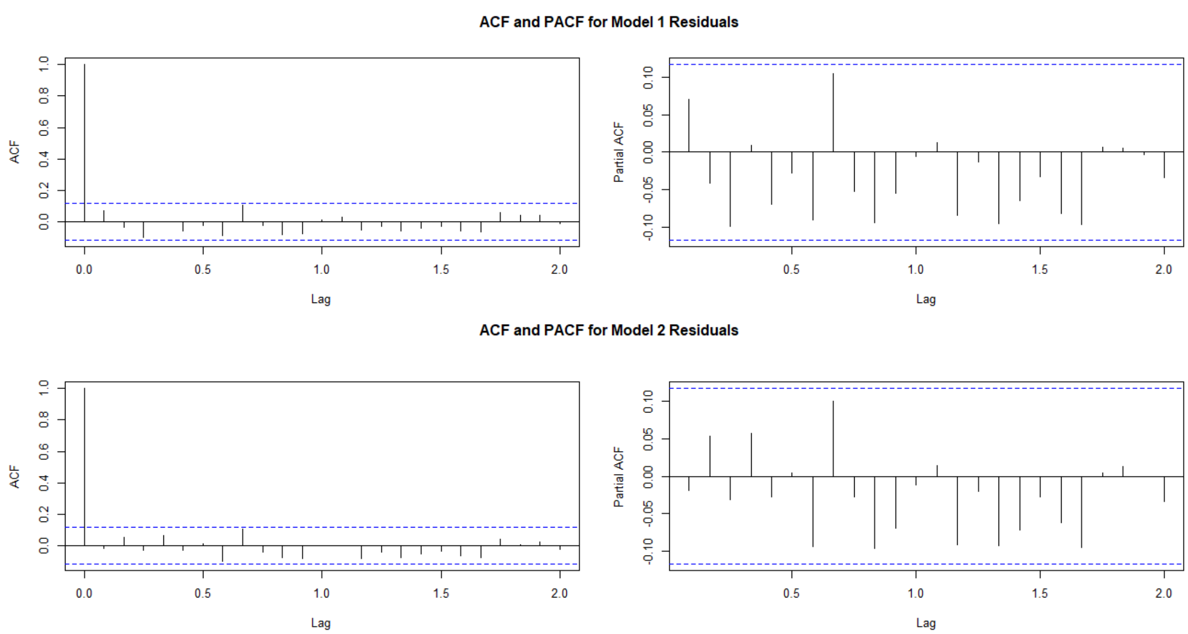

Figure 3: Side by side plots of the sample autocorrelation and sample partial autocorrelation of the model 1 and 2 residuals.

Normal Q-Q plots of the residuals (Figure 12) both indicate fairly normal residuals, with slightly heavy right tails, and both models pass the Shapiro-Wilk test with a p-value of 0.3921 for model 1 and 0.3929 for model 2. Furthermore, plots from the Kolmogorov-Smirnov Test (Figure 13) are within the boundaries for both model residuals, indicating Gaussian white noise. In addition, while both models have p-values greater than 0.05 for Fisher's test, model 1 has a much higher p-value of 0.8297, while model 2 has a lower p-value of 0.3489. This may indicate that model 1 better fits the data than model 2 does. Finally, while both models have p-values greater than 0.05 for Box-Pierce and Ljung-Box tests, model 2 has a passing p-value of 0.0999 for the McLeod-Li test for nonlinear dependence, while model 1 has a p-value of 0.042, which fails the nonlinear dependence test. Since model 1 fails one of our residual tests, we can conclude that model 2 seems to be a more appropriate model for the data. So, our final chosen model is SARIMA$(1,1,1),(0,1,1)_{12}$ with model equation $(1-B)(1-0.2579B)X_t = (1-B^{12})(1-0.7994B)(1-0.8149B^{12})Z_t$.

6 Forecasting

Now that we have decided to model the data with a SARIMA$(1,1,1),(0,1,1)_{12}$ model, we can predict the testing data values to verify that our model can accurately predict future values. The plot of these predicted values superimposed over the evenly spaced data (Figure 14) confirms that our chosen model can very accurately predict the evenly spaced data points. However, our main goal from this report was to predict the original, raw sea level observations. A plot of the predicted test values superimposed over the raw data, provided below, confirms that our model can indeed correctly predict the raw data. The true data, drawn in black, is all within the 95% prediction intervals, drawn in blue, and the exact predicted values, drawn in red, closely follow the true test values.

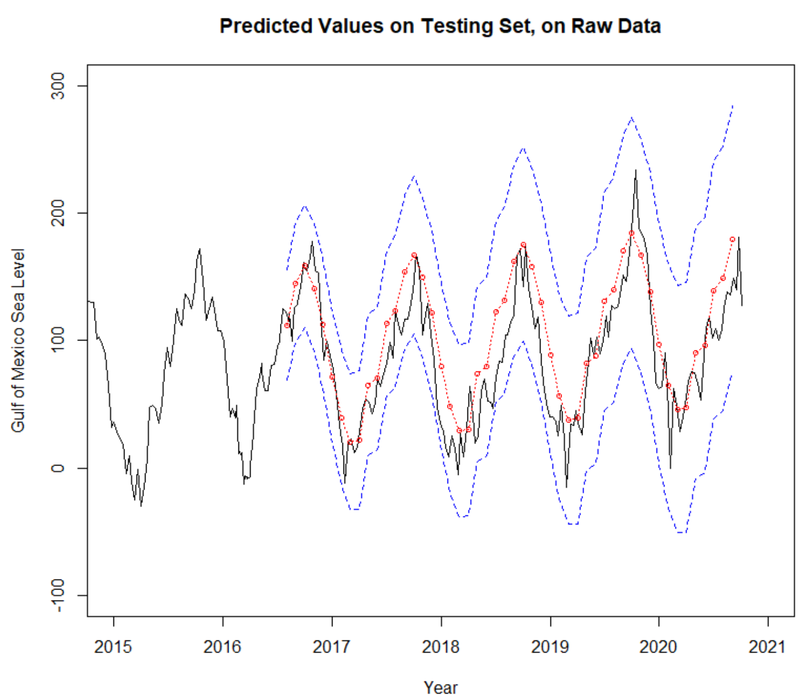

Figure 4: A plot of the raw data, with the predicted test values imposed in red and the confidence intervals imposed in blue.

Now that we have confirmed that our model can accurately predict data, we can use it to predict the change in sea level in the Gulf of Mexico in the next ten years. These predicted values are plotted below, along with 95% prediction intervals. As the prediction year gets larger, the accuracy of prediction decreases, and so the prediction intervals increase. However, based on the accuracy of our test predictions, we can assume that these predictions are fairly accurate. Based on these predictions, the estimated mean sea level of the Gulf of Mexico in October 2030 is 204.4, almost 77 millimeters higher than the observed value of 127 in October 2020.

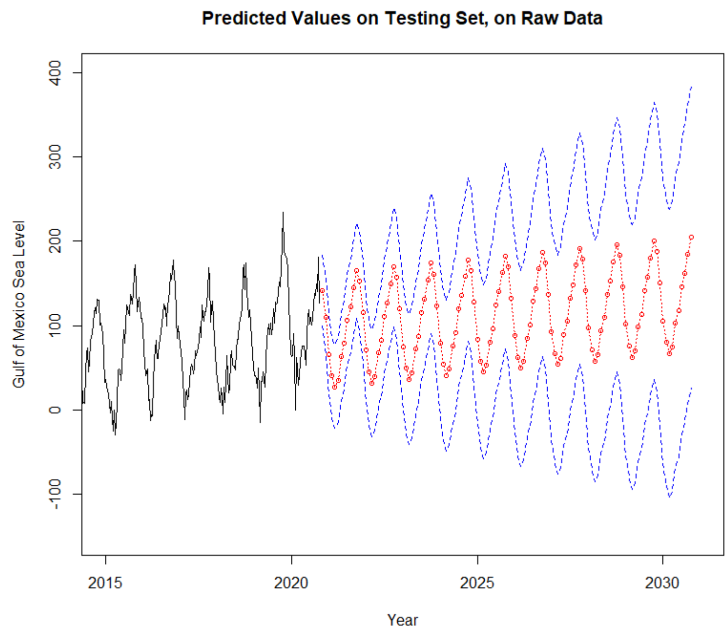

Figure 5: A plot of the raw data, with the predicted future values imposed in red and the confidence intervals imposed in blue.

7 Conclusion

The aim of this report was to identify a time series model to accurately represent the mean sea level change in the Gulf of Mexico, and use this model to predict the changes in the next 10 years. I successfully identified a stationary and invertible SARIMA$(1, 1, 1), (0, 1, 1)_{12}$ model with equation $X_t(1 - 0.2579B) = Z_t(1 - 0.7994B)(1 - 0.8149B^{12})$ that passed all diagnostic checking, and accurately predicted values more than 4 years ahead. Using this model, I predict that in the next 10 years, we can expect to see a 3 inch increase in the mean sea level in the Gulf of Mexico. Policymakers could use this prediction to better prepare for the risks that come with sea level rise, and scientists could use the prediction to develop a more accurate model on how to slow down or reverse the rising sea level.

References

[1] Raisa Feldman. *plot.roots.R*. R Function. 2021.

[2] Christina Nunez. *Sea Level Rise Explained*. Feb. 19, 2019. URL: https://www.nationalgeographic.com/environment/article/sea-level-rise-1.

[3] Coastal Resilience. *Gulf Of Mexico*. URL: https://coastalresilience.org/project/gulf-of-mexico/.

8 Appendix

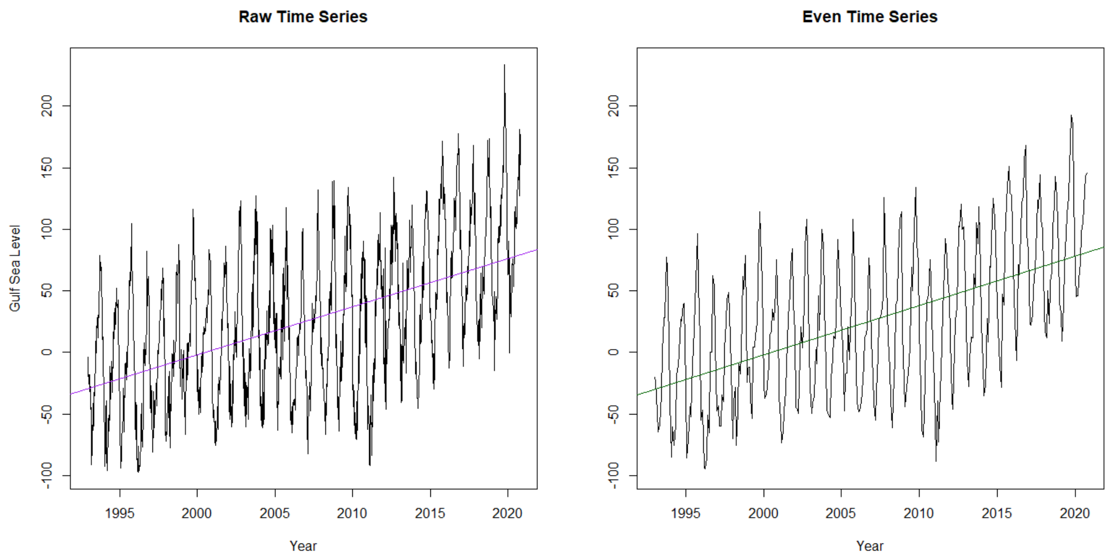

Figure 1: Side by side plots of the raw time series and the time series that was coerced into evenly spaced data points, with linear trends drawn on top.

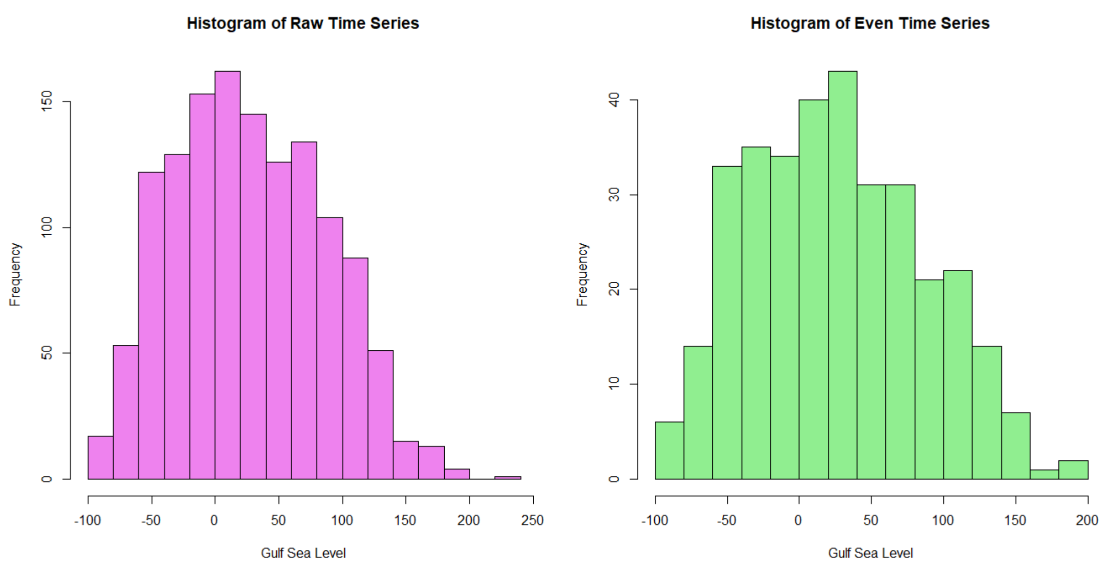

Figure 2: Side by side histograms of the raw time series and the time series that was coerced into evenly spaced data points.

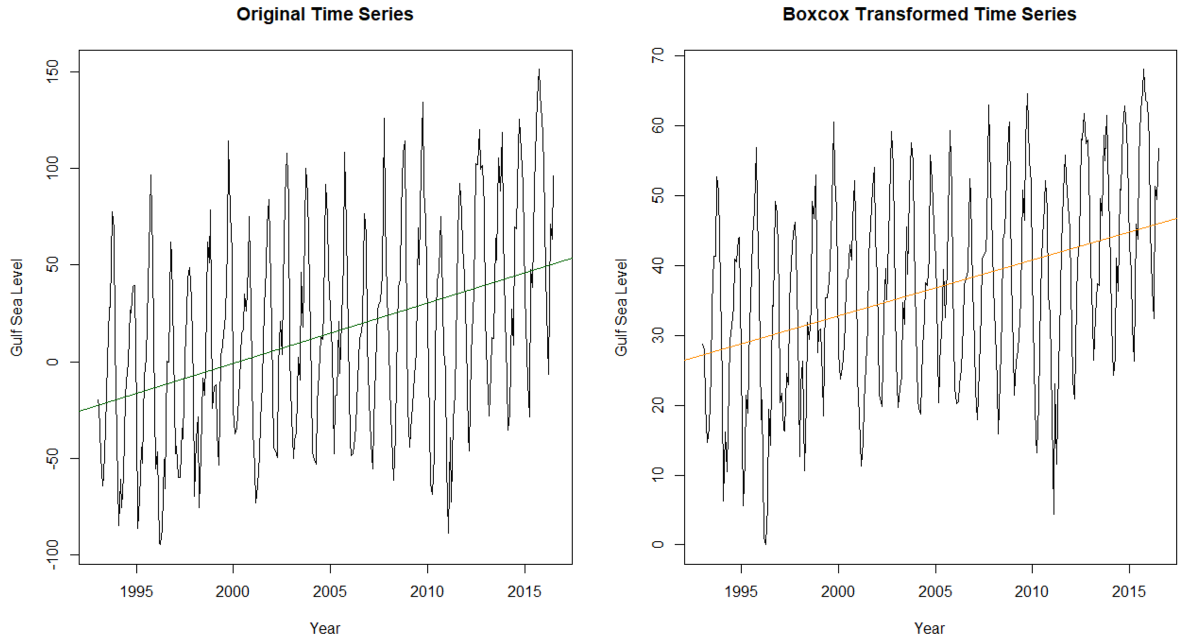

Figure 3: Side by side plots of the non-transformed time series and the Boxcox transformed time series, with linear trends drawn on top.

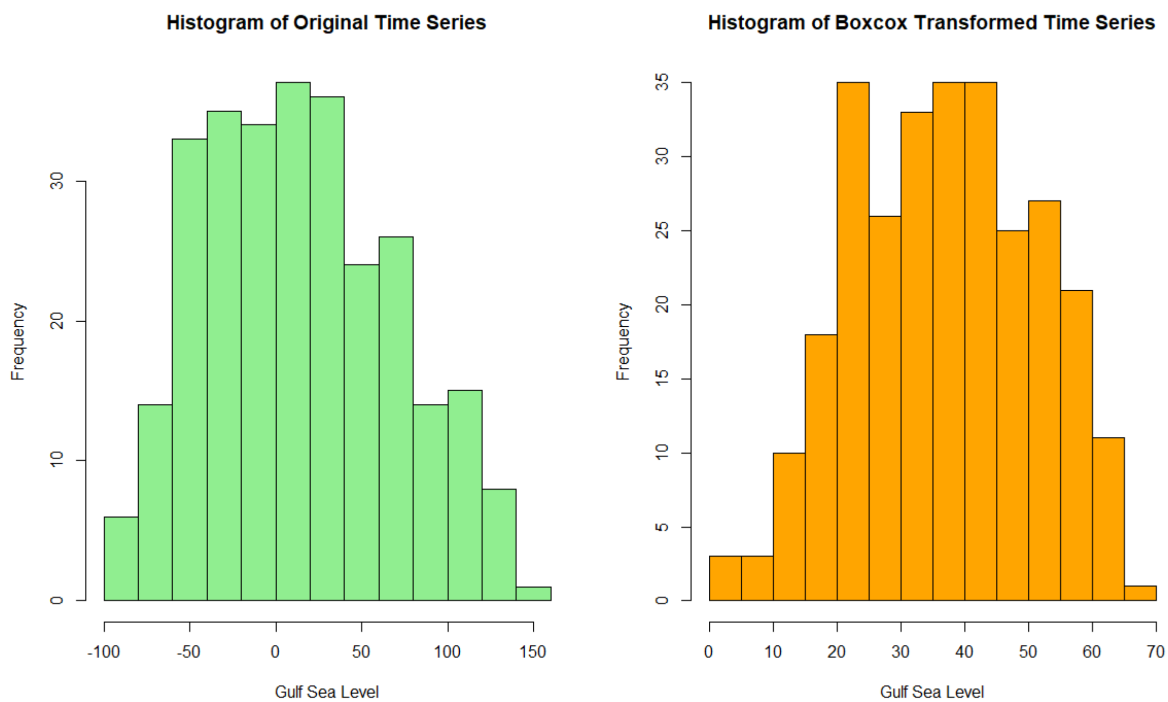

Figure 4: Side by side histograms of the non-transformed time series and the Boxcox transformed time series.

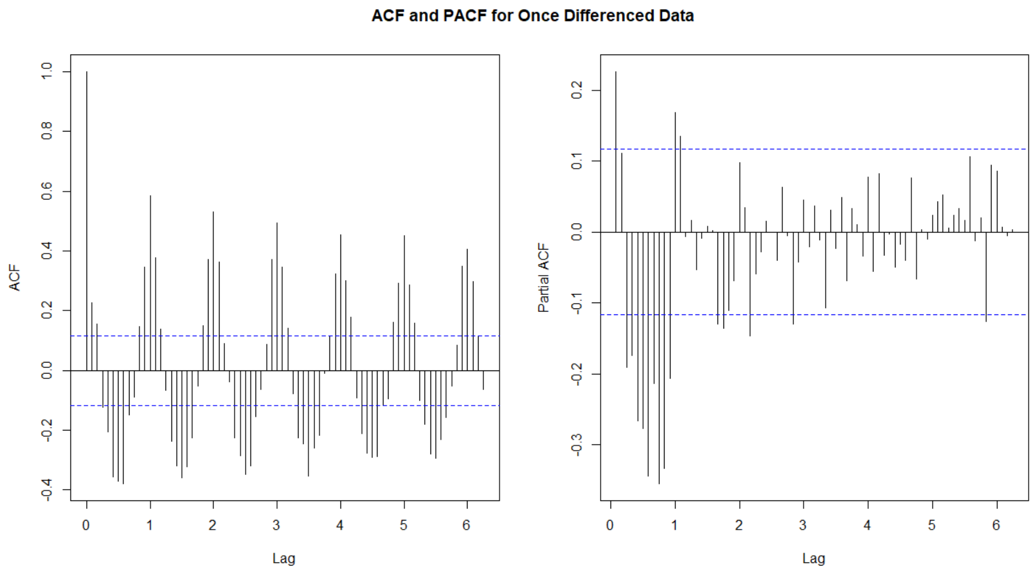

Figure 5: Side by side plots of the sample autocorrelation and sample partial autocorrelation of the data differenced once at lag one.

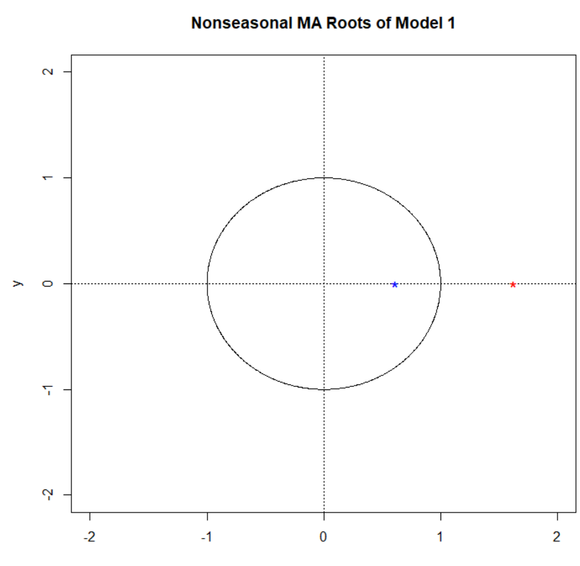

Figure 6: A plot of the unit circle, with the roots of the nonseasonal moving average portion of model 1 drawn in red, and the inverse roots drawn in blue.

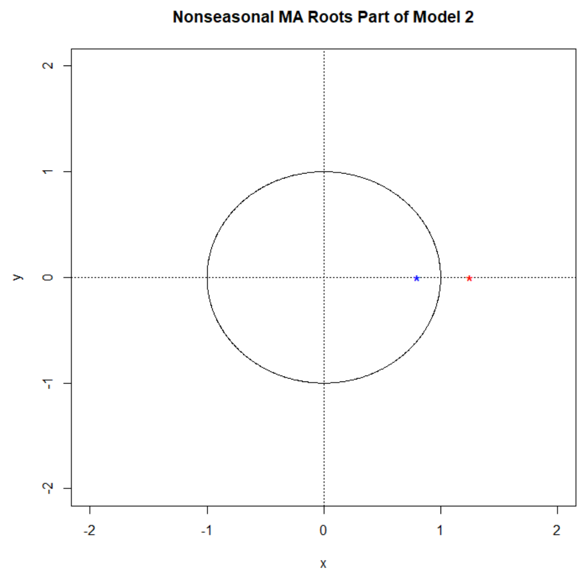

Figure 7: A plot of the unit circle, with the roots of the nonseasonal moving average portion of model 2 drawn in red, and the inverse roots drawn in blue.

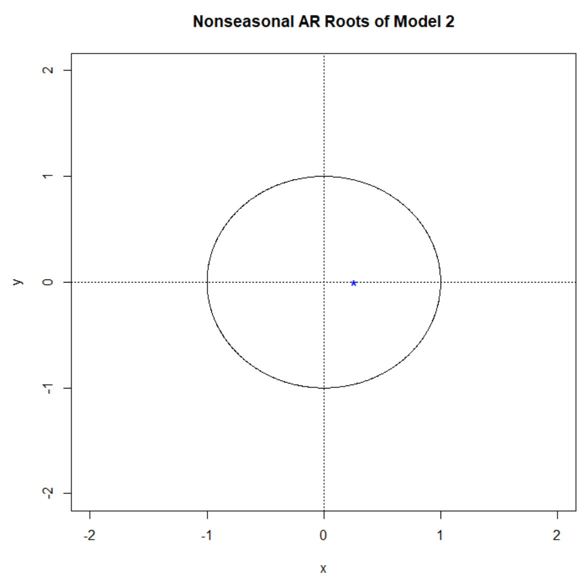

Figure 8: A plot of the unit circle, with the roots of the nonseasonal autoregressive portion of model 2 drawn in red, and the inverse roots drawn in blue.

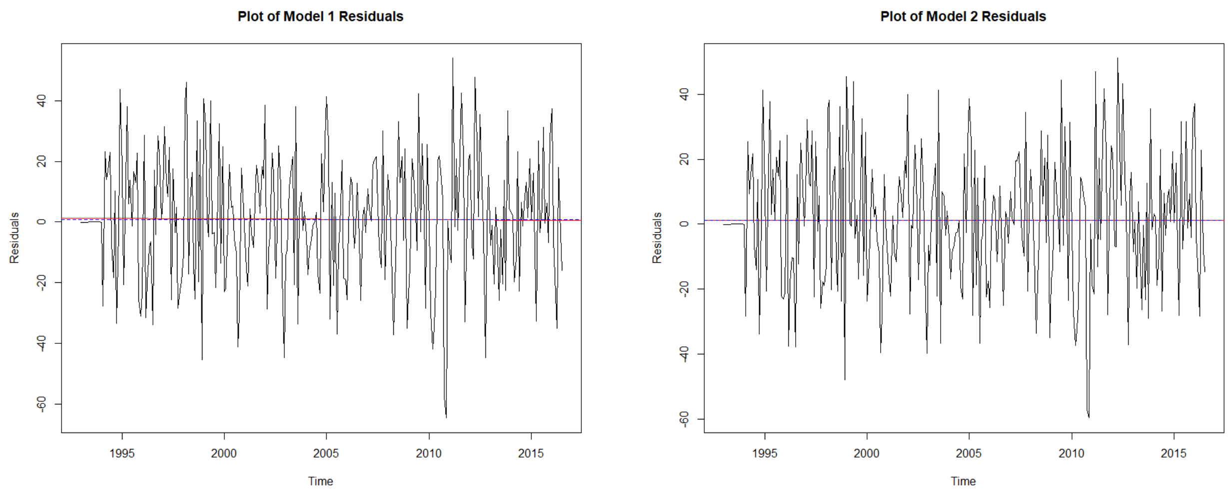

Figure 9: Side by side plots of the residuals of models 1 and 2, with the linear trend drawn in red and the overall mean drawn in blue.

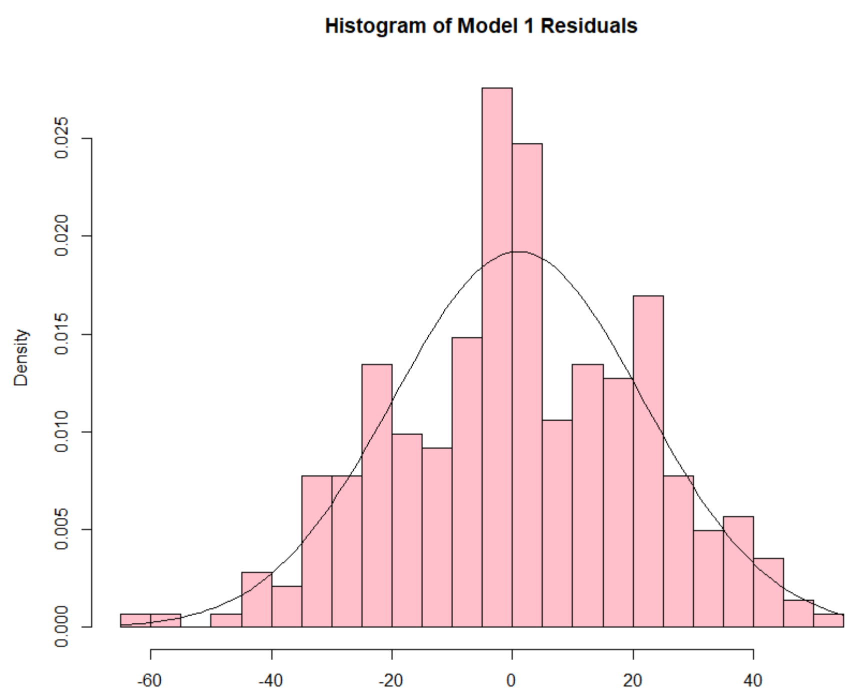

Figure 10: A histogram of the residuals of model 1, with a normal curve superimposed.

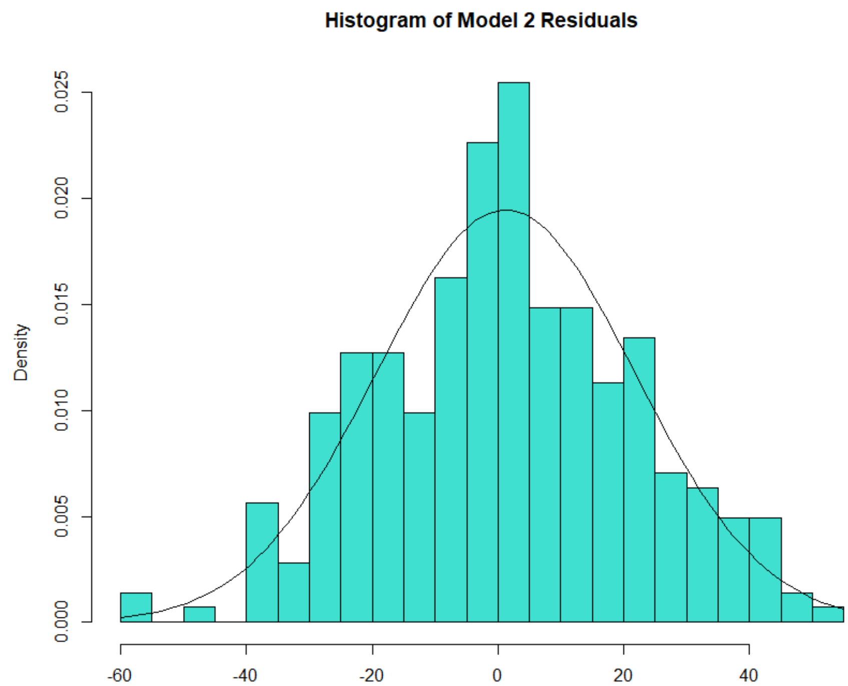

Figure 11: A histogram of the residuals of model 2, with a normal curve superimposed.

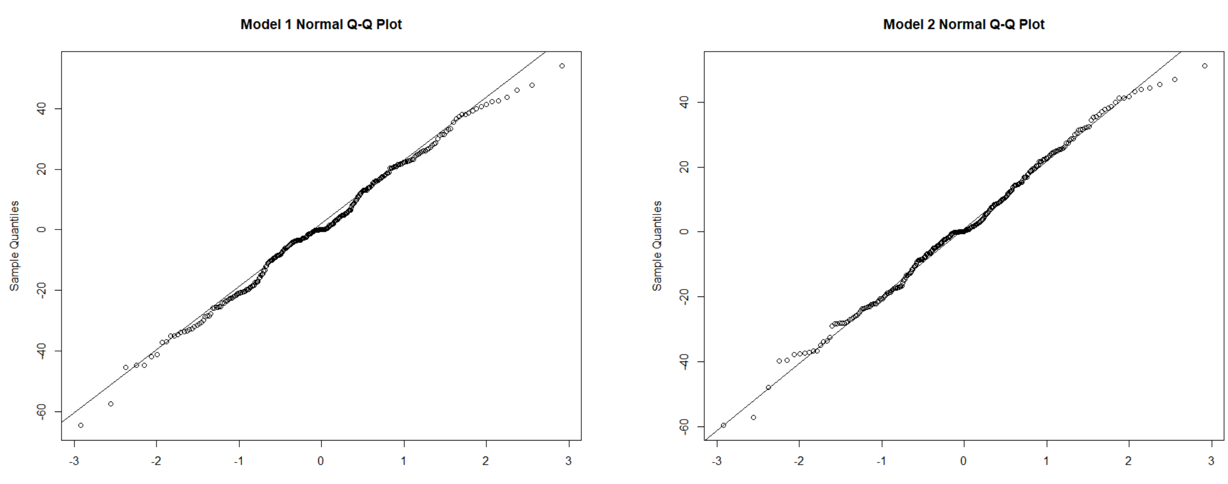

Figure 12: Q-Q Norm plot of the model 1 and 2 residuals.

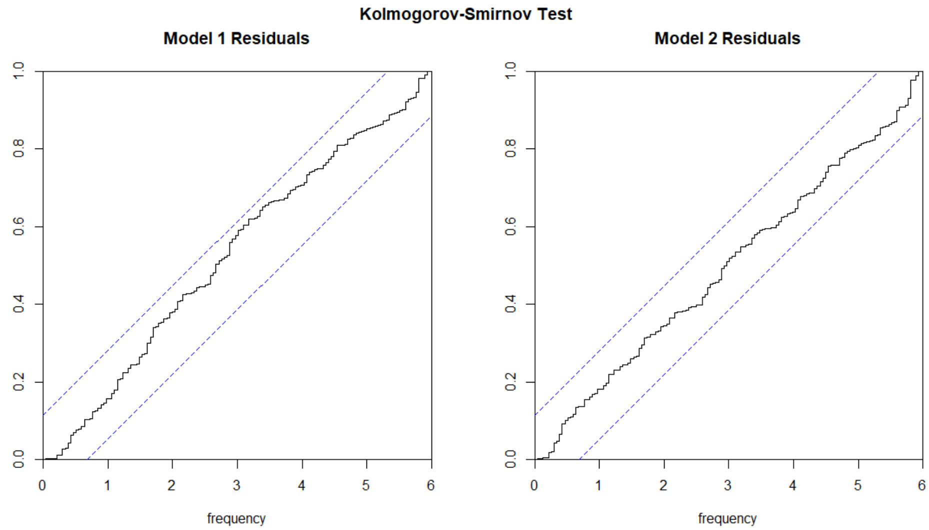

Figure 13: Side by side plots of Kolmogrov-Smirnov Test for model 1 residuals and model 2 residuals.

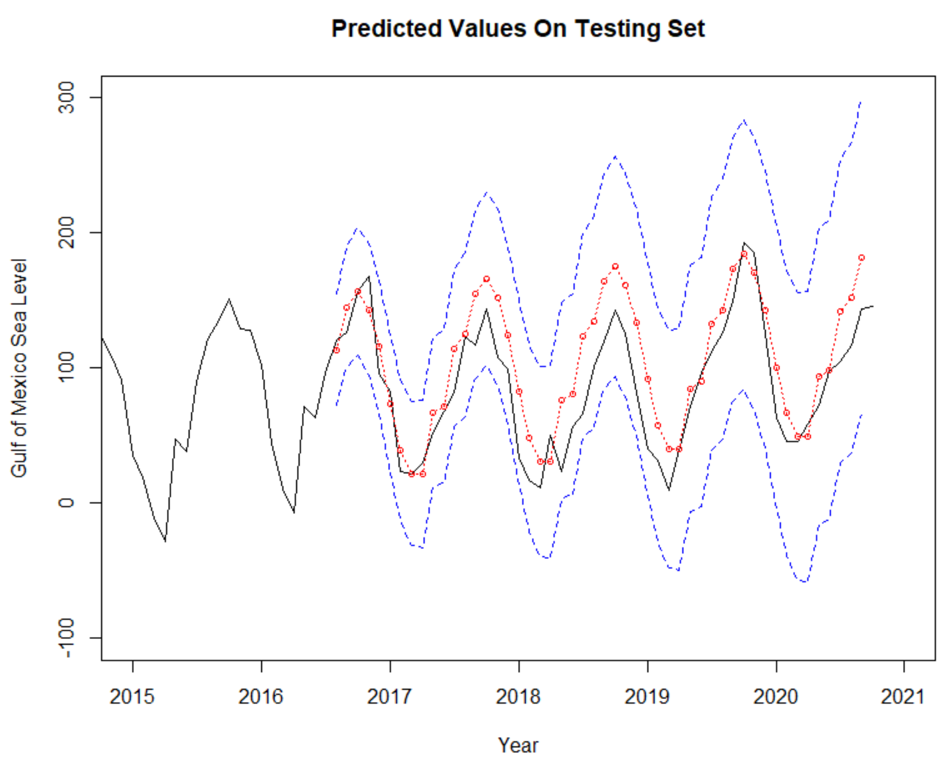

Figure 14: A plot of the original data, with the predicted values imposed in red and the confidence intervals imposed in blue.